Behavior of a Dynamic Covalent Library Driven by Combined Pd(II) and Biphasic Effectors for Metal Transport between Phases

Raphaël Moneuse, Damien Bourgeois, Xavier Le Goff, Jean-marie Lehn, Daniel Meyer

Dynamic behavior of a DCL driven by combined Pd(II) and biphasic effectors for metal transport through between phases

Raphaël Moneuse, Damien Bourgeois, Xavier Le Goff, Jean-Marie Lehn and Daniel Meyer

Dynamic covalent chemistry (DCC) investigates the formation, evolution and behavior of dynamic systems based on the generation of self-assemblies through reversible covalent bonds. These types of systems consist in dynamic covalent libraries (DCLs), *i.e.* a set of building blocks (the components) able to react reversibly with one another to form a distribution of species (the constituents). Being thermodynamically driven, DCLs have the ability to adapt through the modulation of their composition by exchange of components. Various stimuli, either physical or chemical, have been shown to induce a covalent reshuffling of the constituents such as light,[1,2] pH,[3] temperature,[3] medium[4,5] or addition of chemical effectors.[6–12]

Metal cations are common chemical effectors known to initiate a redistribution of the DCL by formation of metal-constituent complexes.[2,4,6–8,10,13,14] Thus, if the kinetics of ligand exchange is rapid enough, the up- or down-regulation of constituents will depend on their affinity with the cation. Almost all studies of the behavior of DCLs in this field have been carried out in single-phase liquid systems. The move to two-phase environments holds out the prospect of various developments not only in the fundamental understanding of DCL behavior in a complex fluid environment, but also in the development of applications such as adaptive liquid-liquid separation. This last point lays the foundations for a genuine paradigm shift in the liquid-liquid extraction of metals through the adaptive in-situ construction of an extractant molecule. However, the effect of a cation in biphasic systems is not as straightforward because of four main reasons. (1) Components and constituents are distributed in the two phases; therefore, they can access two media with different physical properties. It has already been reported with an acetonitrile/water mixture that a phase separation can induce a redistribution of a DCL, promoting the formation of lipophilic and hydrophilic constituents (respectively in the organic phase and water), antagonistic amphiphilic constituents being consumed[5]. (2) Ions have an intrinsic partition coefficient as well and might be found in both phases. (3) DCL and metal cations influence each other; on the one hand, the metal cation induces the redistribution of the DCL by complexation, on the other hand, the composition of the DCL affects the apparent partition coefficient of the metal ion. (4) Phase transfer can be a slow process that may block a distribution in an out-of-equilibrium state. [15]

As mentioned an important application of such biphasic adaptive systems could be the on-demand extraction and separation of metal ions by liquid/liquid extraction. This extraction would be performed by controlling the reorganization of the DCL using either external triggers or the metallic cation itself as chemical effector. The use of DCLs allows the modulation of lipophilicity[8,16] as well as recognition properties[8,11,13,14] (*i.e.* coordination sphere), two key features of liquid/liquid extraction. More specifically, this work will focus on acylhydrazone-based DCLs. Acylhydrazones are a category of Schiff bases that consist in the condensation of an aldehyde and a hydrazide. They are known to be versatile compounds, easily accessible and have complexing properties; as a result, they appear to be promising candidates to generate libraries able to respond to the presence of a metallic cation. Moreover, their formation is reversible and they can undergo reversible transhydrazination reaction. Thus, their dynamic covalent behavior has been exploited in the design of DCLs in numerous studies.[9–11,13,14,17–20]

In previous work, a 1x2 acylhydrazone-based DCL has been developed and investigated with copper(II) nitrate in water/chloroform biphasic system. It was shown that the addition of Cu(II)

triggered a covalent redistribution of the DCL as well as the partial extraction of copper into the organic phase[14]. In the present work, a fourth component was added to this partial DCL (**A1**, **B1** and **B2**), leading to a 2x2 DCL (2 aldehydes and 2 hydrazides). 4-Pyridinecarboxaldehyde was chosen to be the fourth component **A2** for two main reasons (1) **A2** shares a similar structure with **A1**, *i.e*. the pyridine moiety can be protonated, which make its partition coefficient pH-dependent (2) the **A2**-based acylhydrazones formed are not NN-chelate ligands unlike **A1** derivatives (see **FIG. 1.** and **2.**).

Kitamura *et al*. have already reported the synthesis of palladium complexes with *ortho*-pyridine acylhydrazones (**A1** derivatives) as ligands. These species consist in a square planar 1:1 neutral complex with one acylhydrazone coordinating as a NN-bidentate ligand and two chlorides. They have demonstrated that a NNO coordination was possible as well. However, one equivalent of triethylamine is required to deprotonate the acylhydrazone and induce a NNO coordination. Regarding **A2**-based acylhydrazones, two coordination sites are present and lead to different coordination modes: ON bidentate moiety[21–23] and the terminal pyridine.[24]

In this work we studied the behavior of a library of hydrazide and aldehyde components forming potentially acylhydrazone constituents in the presence of Pd(II) in a water-chloroform system.

1/ CHARACTERIZATION OF THE LIBRARY

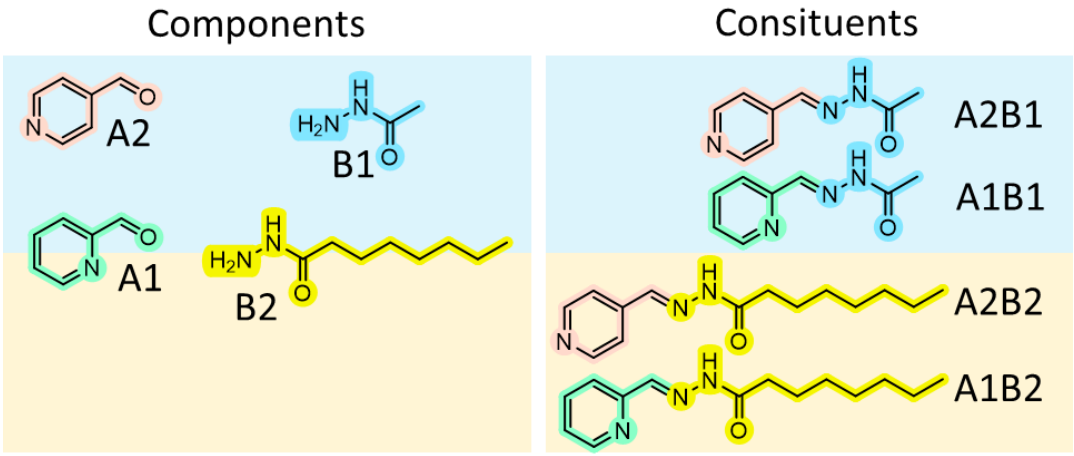

Scheme 1. Representation of the 2x2 DCL. Hydrazide moiety tunes the hydrophobicity and aldehyde controls coordination properties (ONN tridentate vs. ON bidentate). The two colors correspond to the organic phase (yellow) and aqueous phase (blue). The repartition of the eight species, measured at room temperature and pD = 2 (DCl), is illustrated by their position within the two colors (FIG. S1).

Const**i**tuents (corriger)

LIPOPHILICITY OF COMPONENTS AND CONSTITUENTS OF THE LIBRARY

The partition coefficient of components and constituents between the two phases is an important parameter to take into account since it influences the behavior of the DCL and therefore, the efficiency of metallic cation extraction toward the organic phase. This distribution of components between the two phases is expected to have a significant impact on component formation kinetics. The partition coefficients were determined by quantitative ^{1}H-NMR of a D_2O:$CDCl_3$ (1:1, v/v) biphasic system at 50 mM of components/constituents initially dissolved in $CDCl_3$. pD was then adjusted at

pD = 2 with DCl 35% in D_2O. **B1** and **A2B1** are almost exclusively present in water and have a concentration in the organic phase below the limit of detection. Regarding the components, **A2** is hydrophilic (with a partition coefficient of 0.0004) whereas **A1** and **B2** are amphiphilic species (resp. 1.1 and 0.81). Long chain acylhydrazones **A1B2** and **A2B2** are lipophilic (resp. 40 and 6.6). **A1B1** is mainly found in water with a partition coefficient of 0.028. The hydrophilicity of the constituents is controlled by the hydrazide moiety, *i.e.* **B1** tends to drag aldehydes in the water phase. The opposite is also true for **B2** that tends to drag aldehydes in the organic phase (**Scheme 1.**).

STUDY OF THE LIBRARY WITHOUT PALLADIUM

First, the behavior of the DCL by itself was determined. Acylhydrazones are hydrogen bond donors and acceptors thanks to their NH and C=O moieties. This ability to form hydrogen bonds strongly influences their configuration, conformation and aggregation state yielding to chemical shift variations[25,26]. Thus, spectra of **A1B1**, **A1B2**, **A2B1**, and **A2B2** have been recorded in chloroform at different concentrations. Two signals are affected by the concentration variations: NH and azomethine protons. **Tab 1.**, that summarizes chemical shifts of the azomethine proton, was used for signals attribution of acylhydrazones mixtures.

Concentration	**A1B2**	**A2B2**	**A1B1**	**A2B1**
1mM	7.82	7.66	-	-
5mM	7.83	7.70	7.85	7.72
10mM	7.84	7.72	-	-
20mM	7.86	7.76	7.88	7.78
40mM	7.90	7.79	-	-
80mM	7.93	7.83	7.95	7.85

Tab. 1. ^{1}H chemical shifts (ppm) of CH-azomethine proton in CDCl3 at different concentrations

The library was equilibrated in $CDCl_3$ and $CDCl_3/D_2O/DCl$ (pD = 2). Concentration of each specie was determined by quantitative ^{1}H-NMR. The similarity of the four acylhydrazones induces lot of signal overlaps. Azomethine protons produce the only signal that is unique for each specie. Thus, it has been selected as reference for quantification. The distribution of the monophasic experiment in $CDCl_3$ is statistical: 26%/25%/23%/25% (for **A1B1**/**A1B2**/**A2B1**/**A2B2**). A slight redistribution is observed in a biphasic system: 13%/33%/33%/14%, with **A1B1** and **A2B1** being exclusively in the aqueous phase and **A1B2** and **A2B2** in the organic phase. According to **Scheme 1.**, **A1B2** is slightly more lipophilic than **A2B2** and **A1B2** slightly more hydrophilic than **A1B1**. This difference of hydro/lipophilicity could explain the upregulation of **A1B2** and **A2B1** as well as the downregulation of their antagonists **A1B1** and **A2B2**.

2a/ Pd(II) COORDINATION

Complexation properties of acylhydrazones are anticipated to have a strong impact on palladium coordination and extraction efficiency as well as on the behavior of the DCL. Therefore, complexation properties of the constituents have been studied to better understand the effect of Pd(II) on the DCL.

Ortho-pyridine acylhydrazone derivatives (**A1**) were investigated at first. A stoichiometric amount (1:1) of lipophilic **A1B2** was used as to extract Pd(II) from an aqueous phase acidified with HCl (pH = 2). ICP-OES analyses of the organic and aqueous phases show that Pd(II) is transferred to the chloroform phase (>99.9%). ^{1}H-NMR spectrum of this phase confirms the complexation of Pd(II) with **A1B2** by the appearance of a set of new signals and the total disappearance of **A1B2** signature (see FIG. S32-S34). The complex was isolated by evaporation of chloroform and characterized by infrared spectroscopy. Its spectrum shows a characteristic C=O stretching vibration band at 1697 cm^{-1} consistent with the literature[27], suggesting that the oxygen atom of the acylhydrazone is not involved in the coordination (1678 cm^{-1} for the free ligand). ^{15}N-NMR experiment were performed in DMSO to overcome the low solubility of the complex and thus, allow the recording of ^{15}N spectra. Being a hydrogen bond acceptor solvent, DMSO solutions show that both E and Z isomers are observed (two sets of signals). DFT calculations on the two isomers reveal a stabilization of 16.7 kJ/mol in favor of the Z isomer thanks to an intramolecular hydrogen bond. However, in the presence of palladium there is only one set of NMR signals that remains meaning that only one of the two isomers can form a complex with Pd(II). The superimposition of ^{1}H/^{15}N-HMBC (free **A1B2** and the complex) is given in **FIG. 1**. Clearly, only two of the three nitrogen atoms are significantly impacted by the presence of Pd(II): N_{py} and N_{β} with a chemical shift change of respectively 89.9 ppm and 95.6 ppm. The coordination by these two nitrogen atoms is confirmed by a single crystal X-ray diffraction (single crystals obtained by slow evaporation of a chloroform extraction phase). The resulting structure, displayed in **FIG. 1**., shows that the ligand to metal ratio is one and that two cis chloride anions are present in the square planar coordination sphere. To ensure that no other stoichiometries were present in solution, a Job's plot was drawn in DMSO (to solubilize palladium chloride). This plot shows the formation of only one species with a 1:1 palladium to ligand stoichiometry, which is consistent with the X-ray structure.

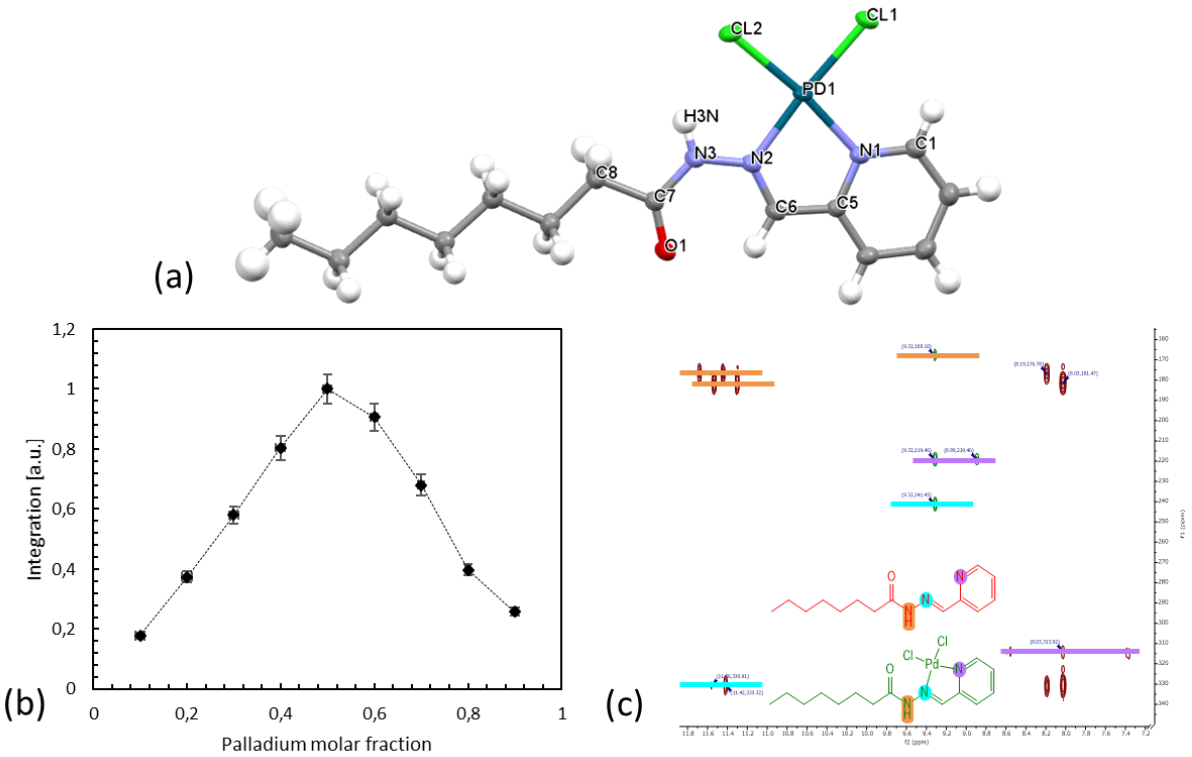

FIG. 1. Characterization of Pd(**A1B2**)Cl_2. (a) Molecular structure obtained by single crystal X-ray diffraction. (b) Job's plot of Pd(**A1B2**)Cl_2. Integration of signal are normalized by the maximum value.

Signals at 9.24 ppm and 8.84 ppm were used and averaged to monitor the complex formation. (c) Superimposition of $^{1}H/^{15}N$-HMBC, free ligand vs. Pd(II) complex.

The same type of complex is formed using the short chain analog **A1B1**, which exhibits the same coordination sphere. All the characterization mentioned before were also carried out on Pd(**A1B1**)Cl_2 except X-ray diffraction. Despite several crystallization attempts using different solvents and techniques (slow evaporation or solvent diffusion) no suitable crystals were obtained. However, three comparable complexes were crystallized successfully from direct slow evaporation of extraction phases. Their X-ray structures are given in **FIG. 1.** and **FIG S55-S56.** and exhibit the same coordination sphere around Pd(II): a square planar geometry (two nitrogen atoms from the ligand and two chloride anions). The structure of the complex with **A1B1** is supposed to be similar to these structures and the structure reported by Kitamura *et al.*[27]

The main difference between these two complexes, beside their lipophilicity, is the solubility in a biphasic system. Lipophilic Pd(**A1B2**)Cl_2 is only found in the chloroform phase whereas Pd(**A1B1**)Cl_2 is neither found in chloroform, nor in water and tends to precipitate out as a yellow crystalline powder.

A comparable methodology was applied to the *para*-pyridine (**A2**) derivatives. A stoichiometric (1:1) amount of lipophilic **A2B2** dissolved in chloroform was used to extract Pd(II) from a 5 mM aqueous solution of palladium chloride (HCl, pH = 2). ICP-OES analyses of the biphasic system show that 50% of Pd(II) is dissolved in each phase. ^{1}H-NMR spectrum reveals a new set of signals as well as the absence of **A2B2** signature. In order to isolate the complex, the extraction was replicated with a higher concentration of palladium and ligand (with the same palladium to ligand ratio). Unlike the low concentration experiment, in this case a yellow solid formed. An elemental analysis of the solute and the precipitate shows a significant difference in composition with a higher percentage of carbon, nitrogen and hydrogen for the solute suggesting a higher ligand to palladium ratio (**Tab. S1.**). ^{1}H- and ^{13}C-NMR spectra of the solute are consistent with the extraction spectra. ^{15}N-NMR experiment were carried out in DMSO for solubility reasons. In this solvent, two sets of ^{15}N signal are observed suggesting that **A2B2** can exist as E- or Z-isomer even after coordination to palladium. Moreover, only N_{py} is significantly shifted. These two observations indicate that **A2B2** is bound two Pd(II) only by the terminal pyridine moiety leaving the acylhydrazone part non coordinated and free to be either E or Z. The IR spectrum shows a characteristic C=O stretching vibration band at 1683 cm^{-1} (1666 cm^{-1} for the free ligand), suggesting that the oxygen atom of the acylhydrazone is not involved in the coordination. Single crystals of the solute were formed by evaporation of chloroform and recrystallization (dioxane/pentane) (**FIG. 2.**). The X-ray structure of these crystals is however not well defined because of the degrees of freedom of the two aliphatic chains. The coordination sphere consists in two ligands **A2B2** and two chloride anions in position trans. This structure is consistent with the conclusion of ^{13}C-and ^{15}N-NMR experiments as well as IR spectra (Supp. Info. Section 4). Regarding the precipitate, its poor solubility in almost all solvents makes its purification difficult. ^{1}H-NMR spectrum in DMSO reveals the presence of Pd(**A2B2**)$_2Cl_2$ as minority product and new signals different from the free ligand. To assess the stoichiometry of this complex, a Job's plot was drawn in DMSO showing the presence of two species: the 1:2-complex characterized earlier (solute) and a 1:1-complex (precipitate). These ligand to metal ratios are consistent with the preliminary elemental analyses showing a higher amount of organic material for the solute. ^{15}N-NMR experiments of the precipitate show a pattern similar to the solute suggesting that **A2B2** is also bound to palladium by the terminal pyridine moiety. Moreover, its IR spectrum shows a characteristic C=O stretching

vibration band as well at 1682 cm^{-1} (1666 cm^{-1} for the free ligand), suggesting that the oxygen atom of the acylhydrazone is not involved in the coordination (Supp. Info. Section 4). Therefore, the insoluble 1:1-complex is supposed to be a palladium dimer with four chloride anions (two of them are involved in a Pd-Pd bridge) and four ligands.

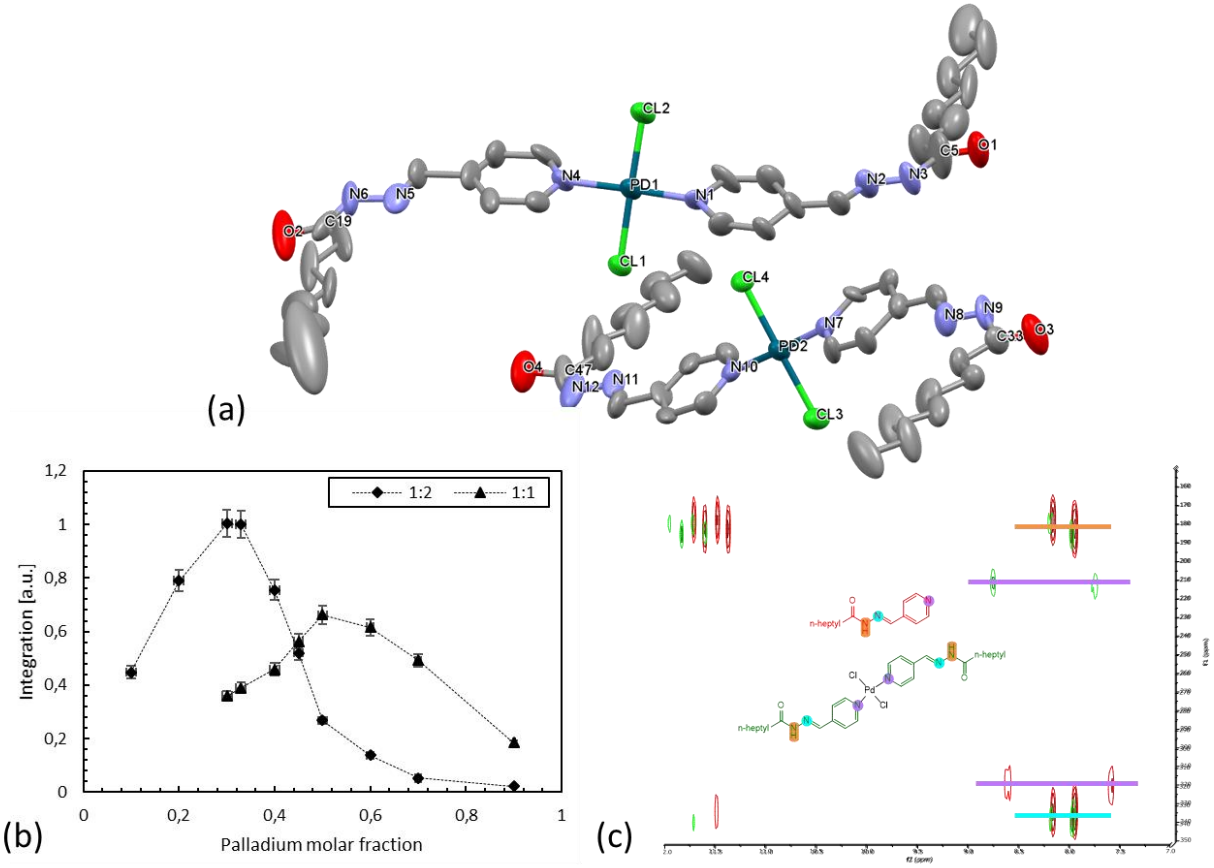

FIG. 2. Characterization of Pd(**A2B2**)$_2$Cl$_2$. (a) Molecular structure obtained by single crystal X-ray diffraction of Pd(**A2B2**)$_2$Cl$_2$. (b) Job's plot of Pd(**A2B2**)$_n$Cl$_2$. Integration of signal are normalized by the maximum value. Signals at 9.24 ppm and 8.84 ppm were used. (c) Superimposition of ^{1}H/^{15}N-HMBC, free ligand vs. Pd(**A2B2**)$_2$Cl$_2$.

Same ^{1}H-, ^{13}C- and ^{15}N-NMR signatures are observed for the short chain analog **A2B1**, suggesting the same type of behavior with Pd(II). The only significant difference is that none of the **A2B1**-based palladium complexes is soluble in water or chloroform.

In biphasic water/chloroform systems with 5 mM Pd(II) concentration, only two types of complexes are observed: 1:1-complexes with **A1**-derivatives and 1:2-complexes with **A2**-derivatives. The lipophilicity of these complexes is dictated by the length chain of the hydrazide moiety.

2b/ DYNAMIC OF EXCHANGE - EFFECT OF PALLADIUM

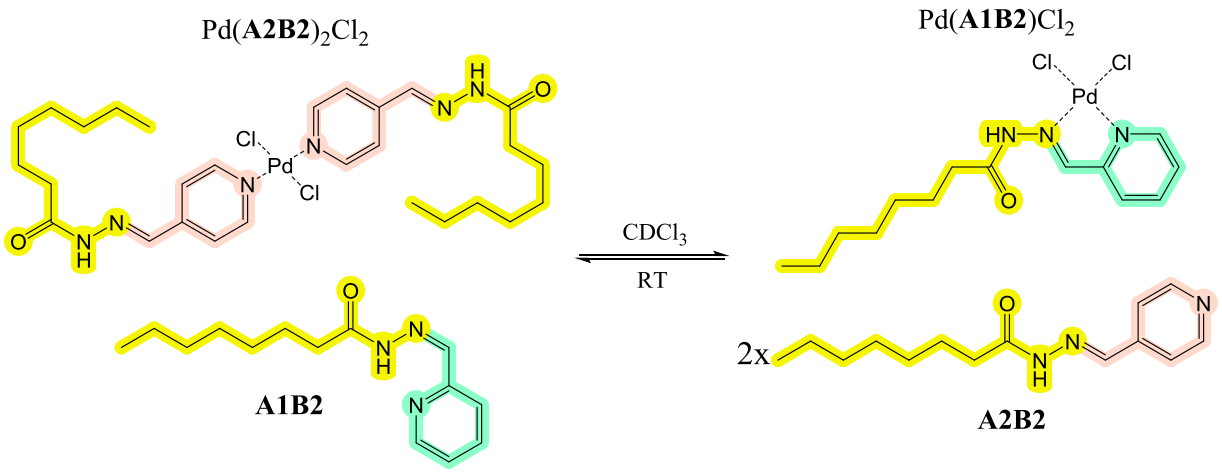

Figure 3. Ligand exchange

In order to ensure a proper redistribution of the library, ligands (constituents) need to be labile enough and complex formation must be reversible. To illustrate this reversibility, ligand exchange was studied in chloroform (see **FIG. 3.**) by ^{1}H-NMR. First, a 5 mM palladium chloride solution (D_2O, DCl, pD = 2) was extracted by a 5 mM $CDCl_3$ solution of **A1B2**. After recovery of the organic phase, two equivalents of **A2B2** were added to the palladium complex Pd(**A1B2**)Cl_2 in solution. ^{1}H-NMR spectra clearly show the formation of Pd(**A2B2**)$_2Cl_2$ and free **A1B2** as well as the consumption of Pd(**A1B2**)Cl_2 and free **A2B2**. The same procedure was done starting from Pd(**A2B2**)$_2Cl_2$ and one equivalent of **A1B2** in solution. Both experiments converged toward the same composition with 50% of each complex in solution after 24 hours (**FIG. S57-S58**).

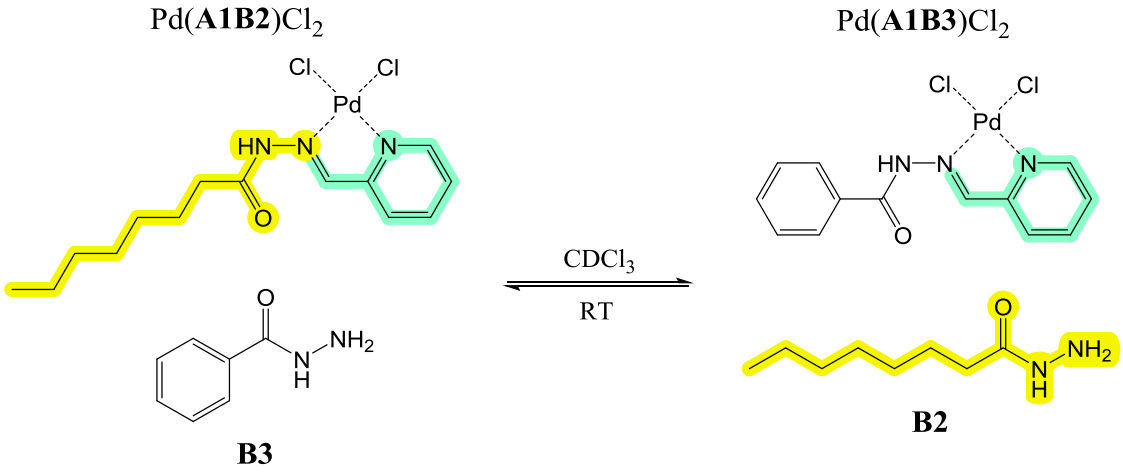

Figure 4. Hydrazide exchange

Similarly, once involved in a complex the C=N bond of an acylhydrazone must remain labile. To study this reversibility, hydrazide-acylhydrazone exchange was performed using solid Pd(**A1B1**)Cl_2 (insoluble in chloroform) and one equivalent of lipophilic **B2** in $CDCl_3$. Exchange is observed but extremely slow, probably due to the fact that the palladium complex is in suspension because of its low solubility. Therefore, another acylhydrazone that generates a soluble palladium complex was used to study this exchange. For this purpose, benzhydrazide was selected and denoted **B3** (see **FIG. 4.**). After the addition of one equivalent of **B3** to the organic phase, Pd(**A1B3**)Cl_2 is formed and Pd(**A1B2**)Cl_2 is partially consumed (see **FIG. 5.**). The same behavior is observed upon the addition of one equivalent of **B2** to a solution of Pd(**A1B3**)Cl_2 leading to a 1:1 mixture of the two palladium complexes (**FIG. S60**).

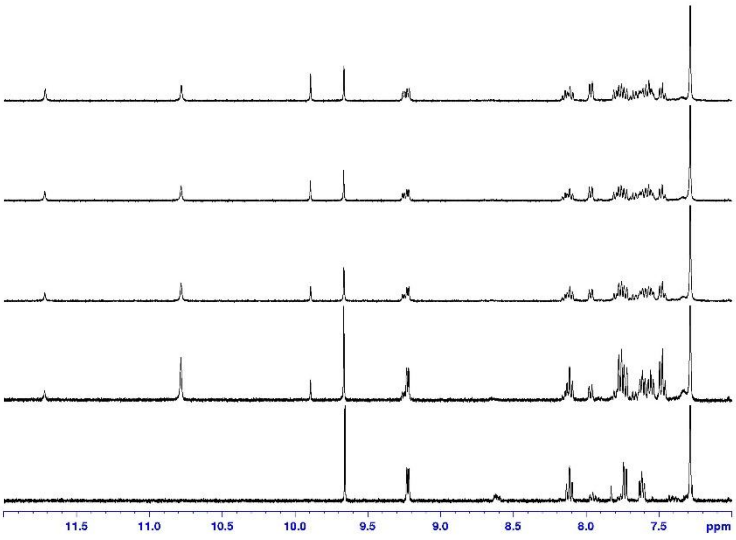

FIG. 5. Hydrazide exchange in chloroform. To a solution of Pd(**A1B2**)Cl_2, one equivalent of **B3** is added. ^1H spectra (restricted to the aromatic region) were recorded over 6 days.

Thus, ligand exchange (24h) is faster than hydrazide exchange (six days). In both cases, the system tends to evolve toward 50%/50% repartition for the two complexes involved in the exchange. Therefore, in monophasic solutions, neither aldehyde moiety nor hydrazide moiety change induces a selection of one unique complex.

3/ 2x2 DYNAMIC COVALENT LIBRARY

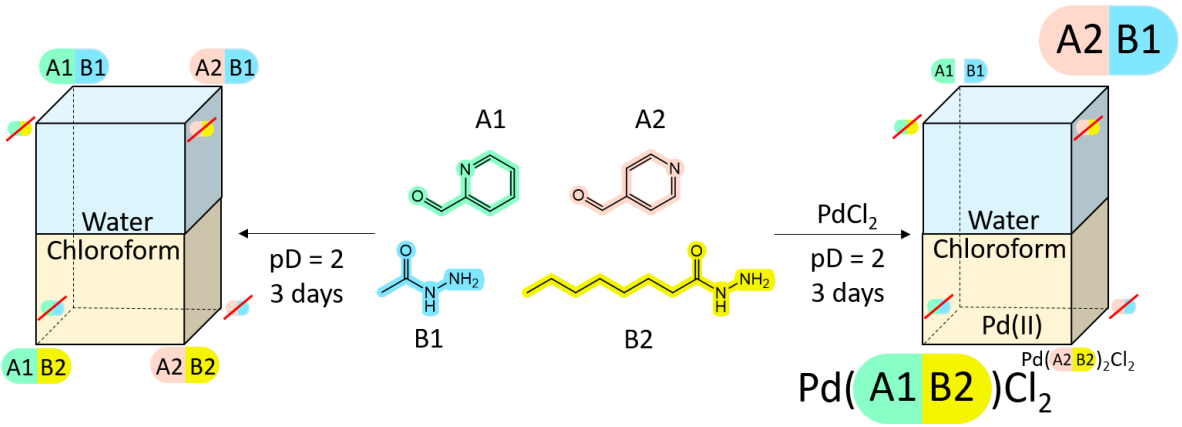

Scheme 2. Structure of the components of the 2x2 DCL. In this representation, each corner corresponds to a constituent. The smallest crossed ovals represent constituents that are under the limit of detection due to hydro/lipophilicity reasons. **A1B1** is depicted as two separate pieces to illustrate hydrolysis.

After having characterized the DCL without Pd(II), coordination properties of the DCL and single-phase exchanges of ligand/hydrazide with Pd(II) that demonstrated its dynamic character in the presence of Pd(II), the behavior of the DCL with Pd(II) in biphasic system was investigated. Upon the addition of a stoichiometric amount of $PdCl_2$ initially to the aqueous phase, the DCL exhibited a strong amplification of **A1B2** in the organic phase with 90% of **A1** being in the form of **A1B2** (either coordinated, 76% or as free ligand, 14%). Pd(II) is not exclusively coordinated to **A1B2**, it can generate a complex with **A2B2** as well (16% of palladium in the form of Pd(**A2B2**)$_2$Cl$_2$). Consequently, Pd(II) is entirely transferred from the aqueous phase to chloroform. **Scheme 2.** depicts these observations: the amplification of **A1B2** and its agonist **A2B1** in the aqueous phase, along the diagonal of the prism. The other diagonal is an illustration of the antagonistic effect, *i.e.* the downregulation of **A1B1** and **A2B2** for the benefit of **A1B2** and **A2B1**.

Conclusion

The results described above lead to several conclusions. The studied 2x2 acylhydrazone-based DCL produces a statistical distribution (25% each) of constituents in single-phase experiment. The equilibrium was usually reached after 5-6 hours. In biphasic systems, the DCL distribution is slightly different. From a thermodynamic point of view, it tends to favor the pair of agonists **A1B2**$_{(org)}$ and **A2B1**$_{(aq)}$, **A1B2** being the most lipophilic and **A2B1** the most hydrophilic constituent of the DCL. This amplification is however relatively weak. From a kinetic point of view, the equilibration is

significantly slower: the equilibrium was reached after 3 days. This behaviour highlights that the kinetics of the single-phase system is mainly ruled by the chemistry whereas in a two-phase system the molecular transport is an important limiting factor.

Under the studied conditions, the presence of Pd(II) leads to two different types of complexes by interacting with this DCL in a water/chloroform biphasic mixture: 1:1 complexes with **A1** derivatives and 1:2 complexes with **A2** derivatives. Single-phase ligand exchange experiments reveal that the two complexes Pd(**A1B2**)Cl_2 and Pd(**A2B2**)$_2Cl_2$ have a comparable stability and show no specific coordination effects. Therefore, moving to a biphasic medium, Pd(II) acts as a chemical effector that triggers the strong up-regulation of **A1B2** through the formation of Pd(**A1B2**)Cl_2. Such behavior illustrates the ability of the DCL to respond to a physical effector (biphasic nature) and a chemical effector (palladium) simultaneously by the amplification of the fittest agonist pair of constituents: **A1B2**$_{(org)}$ and **A2B1**$_{(aq)}$.The DCL studied here allows the total extraction of palladium from the aqueous phase to the organic phase. This extraction is performed by the fittest acylhydrazone, formed *in situ*, that stabilizes palladium into the organic phase. This work contribute to lay down the foundation of a new paradigm to dynamic phase transfer of metal cations for the development of adaptive selective metal cation separation and recovery.

EXPERIMENTAL PART

General procedure.

2-Pyridinecarboxaldehyde, 4-pyridinecarboxaldehyde, acetohydrazide, benzhydrazide, mesitylene and 3-(trimethylsilyl)-1-propanesulfonic acid sodium salt were purchased from Aldrich. Octanehydrazide and palladium(II) chloride were purchased respectively from Accela and Strem. Aldehydes were purified by distillation under reduced pressure and stored under argon.

^{1}H-, ^{13}C-, ^{15}N-NMR spectra were recorded on a Bruker AVANCE NMR (400 MHz) spectrometer. Quantitative NMR were performed using mesitylene and 3-(trimethylsilyl)-1-propanesulfonic acid sodium salt as internal references (resp. in $CDCl_3$ and D_2O). All full spectra are available in supplementary information.

Partition coefficient. A 10 mM solution of mesitylene in $CDCl_3$ and a 50 mM solution of 3-(trimethylsilyl)-1-propanesulfonic acid sodium salt were prepared. Species (50 mM) were dissolved in the mesitylene solution. 4 mL of this $CDCl_3$ solution is contacted with 4 mL of a D_2O solution at pD = 2. pD of the aqueous phase was adjusted at pD = 2 with DCl 35% in D_2O. The biphasic mixture was agitated at room temperature for 15 minutes. The organic phase was analyzed directly by proton NMR. 450 µL of the aqueous phase and 50 µL of the 3-(trimethylsilyl)-1-propanesulfonic acid sodium salt solution were mixed and analyzed by proton NMR as well.

Ligand exchange experiments were conducted at 5 mM. To a 5 mM $CDCl_3$ solution of Pd(**A1B2**)Cl_2 (resp. Pd(**A2B2**)$_2Cl_2$), two equivalents of **A2B2** was added (resp. one equivalent of **A1B2**). The resulting solution was analyzed by proton NMR over six days at room temperature.

Hydrazide exchange experiments were conducted at 5 mM. To a 5 mM $CDCl_3$ solution of Pd(**A1B2**)Cl_2 (resp. Pd(**A1B3**)$_2Cl_2$), one equivalent of **B3** was added (resp. one equivalent of **B2**). The resulting solution was analyzed by proton NMR after one day at room temperature.

DCL experiments. A 10 mM solution of mesitylene in $CDCl_3$ was prepared. 20 mM solutions of **A1**, **A2**, **B1** and **B2** were prepared in the mesitylene solution. A 50 mM solution of 3-(trimethylsilyl)-1-propanesulfonic acid sodium salt were prepared as well.

For the monophasic experiment, 1 mL of each solution was added in a vial resulting in a solution composed of the four components (5 mM). This solution was analyzed by proton NMR after 3 days.

For the biphasic experiment without palladium, the same mixture was prepared. 4 mL of D_2O (pD = 2, DCl) was added to this 4 mL $CDCl_3$ solution. The biphasic mixture was agitated for 3 days at room temperature. The organic phase was analyzed by proton NMR. 450 µL of the

aqueous phase and 50 µL of the 3-(trimethylsilyl)-1-propanesulfonic acid sodium salt solution were mixed and analyzed by proton NMR as well.

For the biphasic experiment without palladium, the same mixture was prepared. 4 mL of a 5 mM $PdCl_2$ solution in D_2O (pD = 2, DCl) was added to this 4 mL $CDCl_3$ solution. The biphasic mixture was agitated for 3 days at room temperature. The organic phase was analyzed by proton NMR. 450 µL of the aqueous phase and 50 µL of the 3-(trimethylsilyl)-1-propanesulfonic acid sodium salt solution were mixed and analyzed by proton NMR as well.

Elemental analyses (Elementar Vario Micro Cube) was conducted at the *plateforme d'analyse et de caractérisation du pôle chimie Balard, Université de Montpellier, France*.

High-resolution mass spectra were recorded on a ThermoFisher Orbitrap Exactive Plus EMR mass spectrometer. Liquid-chromatography coupled with high-resolution mass spectrometry was used in positive mode to determine the composition of the system. The column used for the LC is an Accucore Phenyl-Hexyl 150X2.mm purchased from ThermoFischer and the eluent is acidified acetonitrile HPLC grade (0.1% formic acid), *Institut de science et d'ingénierie supramoléculaire (ISIS), Strasbourg, France*

Palladium concentrations were determined by inductively coupled plasma optical emission spectrometry: ICP-OES, iCAP 7400 Duo Full MFC from Thermo Scientific. Organic phases were back-extracted using a 0.1 mol/L thiourea aqueous solution (HCl pH = 1). For aqueous phases and back-extraction phases, sample were diluted in a nitric (1%) and hydrochloric (1%) acid solution. Calibration curves (0 – 15 mg/L) were prepared from a 1000 mg/L palladium standard solution in 10% HCl (SCP science).

X-ray structural determinations were performed at the *plateforme d'analyse et de caractérisation du pôle chimie Balard, Université de Montpellier, France*. Diffraction data were obtained with a Bruker D8 VENTURE – IµS 3.0 Dual Wavelength spectrometer using Mo radiation (λ = 0.71073 Å).

Fourier Transform Infrared Spectroscopy (FT-IR) was used in Attenuated Total Reflection mode (ATR-FT-IR). FT-IR spectra were recorded using a PerkinElmer Spectrum 100 Spectrometer, operating with a Global MIR source, in combination with a Cesium Iodide (CsI) beam splitter and a deuterated triglycine sulphate DTGS detector, through CsI transmission windows. Spectra were recorded from 615 to 4 000 cm^{-1}, adding 4 scans, using 4 cm^{-1} nominal resolution, operating background correction (atmospheric bands).

Density functional theory (DFT) studies have been performed with Gaussian09 using the B3LYP function.[28] The 6-31G basis set was used for C, H, N, O and Cl, and the SDD basis was used for Pd.

Syntheses

N-(pyridin-2-ylmethylene)octanehydrazide – **A1B2**

To a mixture of 2-pyridinecarboxaldehyde (678 mg, 6.35 mmol, 1.0 eq), octanehydrazide (1.0 g, 6.3 mmol, 1.0 eq) and ethanol (100 mL), TFA (50 µL, 0.63 mmol, 0.1 eq) was added slowly and the resulting mixture was refluxed overnight. Ethanol was distilled off and the solid residue was redissolved in 100 mL of chloroform. The organic phase was washed with 100 mL of a $NaHCO_3$ saturated aqueous solution, then 100 mL of a 1M HCl solution and dried over $MgSO_4$. After filtration, chloroform was evaporated yielding a white solid. Recrystallization from boiling heptane gave *N*-(pyridin-2-ylmethylene)octanehydrazide (1.0 g, 65%) as a white crystalline powder.

^{1}H NMR (400 MHz, $CDCl_3$) δ 9.01 (s, 1H), 8.66 – 8.60 (m, 1H), 7.96 (d, *J* = 8.0 Hz, 1H), 7.87 (s, 1H), 7.76 (td, *J* = 7.8, 1.8 Hz, 1H), 7.35 – 7.27 (m, 1H), 2.83 – 2.75 (m, 2H), 1.76 (p, *J* = 7.5 Hz, 2H), 1.45 – 1.28 (m, 8H), 0.94 – 0.86 (m, 3H)

^{13}C NMR (101 MHz, $CDCl_3$) δ 175.91, 153.02, 149.52, 143.30, 136.52, 124.09, 120.23, 32.70, 31.69, 29.34, 29.07, 24.61, 22.65, 14.10.

HRMS m/z calculated for [$C_{14}H_{21}N_3O+H^+$]: 248.17574, found: 248.17525.

FT-IR ν(C=O): 1678 cm^{-1}

MP 72°C

N-(pyridin-4-ylmethylene)octanehydrazide – **A2B2**

To a mixture of 4-pyridinecarboxaldehyde (678 mg, 6.3 mmol, 1.0 eq), octanehydrazide (1.0 g, 6.3 mmol, 1.0 eq) and dichloromethane (50 mL), solid $MgSO_4$ (3.0 g) was added at once. The suspension was refluxed overnight. After filtration, the solvent was removed under vacuum and the white residue was recrystallized from boiling heptane. *N*-(pyridin-4-ylmethylene)octanehydrazide (1.1 g, 68%) was obtained as a white crystalline powder.

^{1}H NMR (400 MHz, $CDCl_3$) δ 9.72 (s, 1H), 8.72 – 8.66 (m, 2H), 7.76 (s, 1H), 7.62 – 7.51 (m, 2H), 2.79 (t, *J* = 7.6 Hz, 2H), 1.76 (p, *J* = 7.5 Hz, 2H), 1.48 – 1.29 (m, 8H), 0.95 – 0.86 (m, 3H).

^{13}C NMR (101 MHz, $CDCl_3$) δ 177.41, 150.36, 141.30, 140.83, 120.91, 32.72, 31.71, 29.36, 29.04, 24.81, 22.64, 14.09.

HRMS m/z calculated for [$C_{14}H_{21}N_3O+H^+$]: 248.17574, found: 248.17522.

FT-IR ν(C=O): 1667 cm^{-1}

MP 67°C

N-(pyridin-2-ylmethylene)acetohydrazide – **A1B1**

To a mixture of 2-pyridinecarboxaldehyde (1.44 g, 13.5 mmol, 1.0 eq), acetohydrazide (1.1 g, 13.5 mmol, 1.0 eq) and ethanol (100 mL), TFA (70 µL, 0.88 mmol, 0.15 eq) was added slowly and the resulting mixture was refluxed overnight. The blue solution was evaporated. The residue was purified by flash chromatography using dichloromethane/methanol (95:5) as eluent. *N*-(pyridin-2-ylmethylene)acetohydrazide was obtained as a white powder (1.6 g, 63%).

^{1}H NMR (400 MHz, $CDCl_3$) δ 9.10 (s, 1H), 8.64 (dt, *J* = 4.8, 1.4 Hz, 1H), 7.96 (dt, *J* = 8.1, 1.1 Hz, 1H), 7.89 (s, 1H), 7.76 (td, *J* = 7.8, 1.8 Hz, 1H), 7.35 – 7.27 (m, 1H), 2.42 (s, 3H).

^{13}C NMR (101 MHz, $CDCl_3$) δ 173.79, 153.02, 149.57, 143.99, 136.47, 124.10, 120.35, 20.40.

HRMS m/z calculated for [$C_{14}H_{21}N_3O+H^+$]: 164.08184, found: 164.08150.

FT-IR ν(C=O): 1662 cm^{-1}

MP 125°C

N-(pyridin-4-ylmethylene)acetohydrazide – **A2B1**

Acetohydrazide (540 mg, 7.3 mmol, 1.0 eq) and 4-pyridinecarboxaldehyde (780 mg, 7.3 mmol, 1.0 eq) were directly combined in a mortar. The reaction was carried out without solvent: the reactant were manually stirred with a pestle for 10 minutes until the slurry solidifies.[14] Purification of the white solid by flash chromatography using dichloromethane/methanol (95:5) as eluent. N-(pyridin-4-ylmethylene)acetohydrazide was obtained as a white powder (643 mg, 54%).

^{1}H NMR (400 MHz, $CDCl_3$) δ 10.88 (s, 1H), 8.71 – 8.63 (m, 2H), 7.86 (s, 1H), 7.60 – 7.52 (m, 2H), 2.43 (s, 3H).

^{13}C NMR (101 MHz, $CDCl_3$) δ 174.90, 150.39, 141.28, 141.15, 120.92, 20.35.

HRMS m/z calculated for [$C_{14}H_{21}N_3O+H^+$]: 164.08184, found: 164.08164.

FT-IR ν(C=O): 1685 cm^{-1}

MP 166°C

N-(pyridin-2-ylmethylene)benzohydrazide – **A1B3**

A mixture of 2-pyridinecarboxaldehyde (793 mg, 7.4 mmol, 1.0 eq), benzhydrazide (1.0 g, 7.4 mmol, 1.0 eq) and ethanol (100 mL) was refluxed overnight. The solvent was removed under vacuum and the white residue was recrystallized from a toluene/DMSO mixture (99:1). Crystals were washed twice with 20 mL of Et_2O. *N*-(pyridin-2-ylmethylene)benzohydrazide was obtained as a white crystalline powder (981 mg, 59%).

^{1}H NMR (400 MHz, MeOD) δ 8.59 (d, *J* = 5.0 Hz, 1H), 8.43 (s, 1H), 8.34 (d, *J* = 8.0 Hz, 1H), 7.98 (d, *J* = 7.6 Hz, 2H), 7.93 (t, *J* = 7.8 Hz, 1H), 7.64 (dd, *J* = 8.4, 6.4 Hz, 1H), 7.55 (t, *J* = 7.7 Hz, 2H), 7.50 – 7.42 (m, 1H).

^{13}C NMR (101 MHz, MeOD) δ 165.93, 153.12, 148.77, 147.98, 137.26, 132.44, 132.19, 128.40, 127.52, 124.67, 120.94.

HRMS m/z calculated for [$C_{13}H_{11}N_3O+H^+$]: 226.09749, found: 226.09684.

FT-IR ν(C=O): 1658 cm^{-1}

MP 110°C

N-(pyridin-2-ylmethylene)butanehydrazide – **A1B4**

To a mixture of 4-pyridinecarboxaldehyde (1.1 g, 10.4 mmol, 1.0 eq), butanehydrazide (1.1 g, 10.4 mmol, 1.0 eq) and dichloromethane (100 mL), solid $MgSO_4$ (3.0 g) was added at once. The suspension was refluxed overnight. After filtration, the solvent was removed under vacuum and the white residue was recrystallized from ethanol. *N*-(pyridin-2-ylmethylene)butanehydrazide was obtained as a white crystalline material (1.67 g, 84%).

^{1}H NMR (400 MHz, $CDCl_3$) δ 8.91 (s, 1H), 8.63 (ddd, *J* = 4.9, 1.6, 0.9 Hz, 1H), 7.97 (dt, *J* = 7.9, 0.9 Hz, 1H), 7.85 (s, 1H), 7.76 (td, *J* = 7.8, 1.6 Hz, 1H), 7.31 (ddd, *J* = 7.8, 4.9, 1.1 Hz, 1H), 2.78 (t, *J* = 7.6 Hz, 2H), 1.80 (h, *J* = 7.6 Hz, 2H), 1.06 (t, *J* = 7.4 Hz, 3H).

^{13}C NMR (101 MHz, $CDCl_3$) δ 176.25, 153.17, 149.52, 143.65, 136.46, 124.02, 121.28, 120.26, 34.54, 18.06, 13.97.

HRMS m/z calculated for [$C_{10}H_{13}N_3O+H^+$]: 192.11314, found: 192.11257.

FT-IR ν(C=O): 1667 cm^{-1}

MP 104°C

Pd(**A1B2**)Cl_2

Palladium chloride (168.5 mg, 0.95 mmol, 1.0 eq) was dissolved in 40 mL of water (pH = 1, HCl). A1B2 (225.5 mg, 0.91 mmol, 1.0 eq) was dissolved in 40 mL of chloroform. The A1B2 chloroform solution was added to the aqueous palladium solution. The biphasic mixture was stirred for 1h at room temperature. The organic phase was recovered, dried over $MgSO_4$ and evaporated *in vacuo*. Complex was collected as a yellow powder (292 mg, 74%).

^{1}H NMR (400 MHz, $CDCl_3$) δ 10.72 (s, 1H), 9.66 (s, 1H), 9.19 (d, *J* = 5.4 Hz, 1H), 8.12 (t, *J* = 7.8 Hz, 1H), 7.76 (d, *J* = 7.9 Hz, 1H), 7.61 (t, *J* = 7.8 Hz, 1H), 2.42 (t, *J* = 7.6 Hz, 2H), 1.72 (p, *J* = 7.2 Hz, 2H), 1.44 – 1.21 (m, 8H), 0.97 – 0.84 (m, 3H).

^{13}C NMR (101 MHz, $CDCl_3$) δ 171.71, 156.40, 152.86, 151.23, 140.58, 126.75, 126.35, 35.84, 31.58, 28.96, 28.84, 24.83, 22.57, 14.06.

Elemental analysis calculated (%) for $C_{14}H_{21}Cl_2N_3OPd$: C, 39.59; H, 4.98; N, 9.89; found: C, 40.11; H, 5.36; N, 9.83

FT-IR ν(C=O): 1697 cm^{-1}

Pd(**A1B3**)Cl_2

Palladium chloride (100.0 mg, 0.56 mmol, 1.0 eq) was dissolved in 20 mL of water (pH = 1, HCl). A1B4 (126.0 mg, 0.56 mmol, 1.0 eq) was dissolved in 100 mL of chloroform. The A1B2 chloroform solution was added to the aqueous palladium solution. The biphasic mixture was stirred for 1h at room temperature. The organic phase was recovered, dried over $MgSO_4$ and evaporated *in vacuo*. Complex was collected as a yellow powder (160 mg, 71%).

^{1}H NMR (400 MHz, $CDCl_3$) δ 11.72 (s, 1H), 9.89 (s, 1H), 9.25 (d, *J* = 5.6 Hz, 1H), 8.14 (td, *J* = 7.8, 1.5 Hz, 1H), 7.98 – 7.94 (m, 2H), 7.80 (d, *J* = 7.8 Hz, 1H), 7.70 – 7.61 (m, 2H), 7.59 – 7.54 (m, 2H).

^{13}C NMR (101 MHz, $CDCl_3$) δ 164.84, 156.42, 152.40, 151.40, 140.47, 133.90, 130.68, 129.38, 127.65, 126.77, 126.24.

FT-IR ν(C=O): 1682 cm^{-1}

Pd(**A1B4**)Cl_2

Palladium chloride (100.0 mg, 0.56 mmol, 1.0 eq) was dissolved in 20 mL of water (pH = 1, HCl). A1B4 (108.0 mg, 0.56 mmol, 1.0 eq) was dissolved in 100 mL of chloroform. The A1B2 chloroform solution was added to the aqueous palladium solution. The biphasic mixture was stirred for 1h at room temperature. The organic phase was recovered, dried over $MgSO_4$ and evaporated *in vacuo*. Complex was collected as a yellow powder (197.2 mg, 90%).

^{1}H NMR (400 MHz, $CDCl_3$) δ 10.73 (s, 1H), 9.66 (s, 1H), 9.18 (d, *J* = 5.7 Hz, 1H), 8.12 (td, *J* = 7.8, 1.5 Hz, 1H), 7.76 (d, *J* = 7.9 Hz, 1H), 7.61 (td, *J* = 6.7, 1.4 Hz, 1H), 2.42 (t, *J* = 7.5 Hz, 2H), 1.77 (h, *J* = 7.4 Hz, 2H), 1.03 (t, *J* = 7.4 Hz, 3H).

^{13}C NMR (101 MHz, $CDCl_3$) δ 171.53, 156.38, 152.84, 151.26, 140.52, 126.75, 126.32, 37.66, 18.41, 13.56.

FT-IR ν(C=O): 1694 cm^{-1}

Pd(**A1B1**)Cl_2

Palladium chloride (168.5 mg, 0.95 mmol, 1.0 eq) was dissolved in 40 mL of water (pH = 1, HCl). A1B1 (155 mg, 0.95 mmol, 1.0 eq) was dissolved in 20 mL of water (pH = 1, HCl). The A1B1 aqueous solution was added to the aqueous palladium solution. The resulting suspension was stirred for 1h at room temperature and centrifuged to remove the supernatant. The residue was washed twice with 10 mL of ethanol and a light yellow solid was obtained (197 mg, 62%).

^{1}H NMR (400 MHz, DMSO-*d*6) δ 10.62 (s, 1H), 9.29 (s, 1H), 8.90 (d, *J* = 5.4 Hz, 1H), 8.34 (t, *J* = 7.8 Hz, 1H), 8.23 (d, *J* = 7.7 Hz, 1H), 7.35 (t, *J* = 6.8 Hz, 1H), 2.15 (s, 3H).

FT-IR ν(C=O): 1713 cm^{-1}

References

(1) Ingerman, L. A.; Waters, M. L. Photoswitchable Dynamic Combinatorial Libraries: Coupling Azobenzene Photoisomerization with Hydrazone Exchange. *J. Org. Chem.* **2009**, *74* (1), 111–117. https://doi.org/10.1021/jo801783w.

(2) Vantomme, G.; Lehn, J.-M. Reversible Adaptation to Photoinduced Shape Switching by Oligomer–Macrocycle Interconversion with Component Selection in a Three-State Constitutional Dynamic System. *Chem. – Eur. J.* **2014**, *20* (49), 16188–16193. https://doi.org/10.1002/chem.201404561.

(3) Giuseppone, N.; Lehn, J.-M. Protonic and Temperature Modulation of Constituent Expression by Component Selection in a Dynamic Combinatorial Library of Imines. *Chem. - Eur. J.* **2006**, *12* (6), 1715–1722. https://doi.org/10.1002/chem.200501038.

(4) Ramírez, J.; Stadler, A.-M.; Kyritsakas, N.; Lehn, J.-M. Solvent-Modulated Reversible Conversion of a [2×2]-Grid into a Pincer-like Complex. *Chem Commun* **2007**, No. 3, 237–239. https://doi.org/10.1039/B612222A.

(5) Hafezi, N.; Lehn, J.-M. Adaptation of Dynamic Covalent Systems of Imine Constituents to Medium Change by Component Redistribution under Reversible Phase Separation. *J. Am. Chem. Soc.* **2012**, *134* (30), 12861–12868. https://doi.org/10.1021/ja305379c.

(6) Men, G.; Lehn, J.-M. Higher Order Constitutional Dynamic Networks: [2×3] and [3×3] Networks Displaying Multiple, Synergistic and Competitive Hierarchical Adaptation. *J. Am. Chem. Soc.* **2017**, *139* (6), 2474–2483. https://doi.org/10.1021/jacs.6b13072.

(7) Holub, J.; Vantomme, G.; Lehn, J.-M. Training a Constitutional Dynamic Network for Effector Recognition: Storage, Recall, and Erasing of Information. *J. Am. Chem. Soc.* **2016**, *138* (36), 11783–11791. https://doi.org/10.1021/jacs.6b05785.

(8) Vantomme, G.; Jiang, S.; Lehn, J.-M. Adaptation in Constitutional Dynamic Libraries and Networks, Switching between Orthogonal Metalloselection and Photoselection Processes. *J. Am. Chem. Soc.* **2014**, *136* (26), 9509–9518. https://doi.org/10.1021/ja504813r.

(9) Lam, R. T. S.; Belenguer, A.; Roberts, S. L.; Naumann, C.; Jarrosson, T.; Otto, S.; Sanders, J. K. M. Amplification of Acetylcholine-Binding Catenanes from Dynamic Combinatorial Libraries. *Science* **2005**, *308* (5722), 667–669. https://doi.org/10.1126/science.1109999.

(10) Dhers, S.; Holub, J.; Lehn, J.-M. Coevolution and Ratiometric Behaviour in Metal Cation-Driven Dynamic Covalent Systems. *Chem. Sci.* **2017**, *8* (3), 2125–2130. https://doi.org/10.1039/C6SC04662B.

(11) Klein, J. M.; Saggiomo, V.; Reck, L.; Lüning, U.; Sanders, J. K. M. Dynamic Combinatorial Libraries for the Recognition of Heavy Metal Ions. *Org Biomol Chem* **2012**, *10* (1), 60–66. https://doi.org/10.1039/C1OB05976A.
(12) Shen, L.; Cao, N.; Tong, L.; Zhang, X.; Wu, G.; Jiao, T.; Yin, Q.; Zhu, J.; Pan, Y.; Li, H. Dynamic Covalent Self-Assembly Based on Oxime Condensation. *Angew. Chem.* **2018**, *130* (50), 16724–16728. https://doi.org/10.1002/ange.201811025.
(13) Men, G.; Lehn, J.-M. Multiple Adaptation of Constitutional Dynamic Networks and Information Storage in Constitutional Distributions of Acylhydrazones. *Chem. Sci.* **2019**, *10* (1), 90–98. https://doi.org/10.1039/C8SC03858A.
(14) Chevalier, A.; Osypenko, A.; Lehn, J.-M.; Meyer, D. Phase Transfer of Metal Cations by Induced Dynamic Carrier Agents: Biphasic Extraction Based on Dynamic Covalent Chemistry. *Chem. Sci.* **2020**, 10.1039.D0SC04098C. https://doi.org/10.1039/D0SC04098C.
(15) Lehn, J.-M. Perspectives in Chemistry-Aspects of Adaptive Chemistry and Materials. *Angew. Chem. Int. Ed.* **2015**, *54* (11), 3276–3289. https://doi.org/10.1002/anie.201409399.
(16) Vantomme, G.; Hafezi, N.; Lehn, J.-M. A Light-Induced Reversible Phase Separation and Its Coupling to a Dynamic Library of Imines. *Chem Sci* **2014**, *5* (4), 1475–1483. https://doi.org/10.1039/C3SC53130A.
(17) Simpson, M. G.; Pittelkow, M.; Watson, S. P.; Sanders, J. K. M. Dynamic Combinatorial Chemistry with Hydrazones: Cholate-Based Building Blocks and Libraries. *Org. Biomol. Chem.* **2010**, *8* (5), 1173. https://doi.org/10.1039/b917145b.
(18) Choudhary, S.; Morrow, J. R. Dynamic Acylhydrazone Metal Ion Complex Libraries: A Mixed–Ligand Approach to Increased Selectivity in Extraction. *Angew. Chem.* **2002**, *114* (21), 4270–4272. https://doi.org/10.1002/1521-3757(20021104)114:21<4270::AID-ANGE4270>3.0.CO;2-7.
(19) Bhat, V. T.; Caniard, A. M.; Luksch, T.; Brenk, R.; Campopiano, D. J.; Greaney, M. F. Nucleophilic Catalysis of Acylhydrazone Equilibration for Protein-Directed Dynamic Covalent Chemistry. *Nat. Chem.* **2010**, *2* (6), 490–497. https://doi.org/10.1038/nchem.658.
(20) Barsoum, D. N.; Kirinda, V. C.; Kang, B.; Kalow, J. A. Remote-Controlled Exchange Rates by Photoswitchable Internal Catalysis of Dynamic Covalent Bonds. *J. Am. Chem. Soc.* **2022**, *144* (23), 10168–10173. https://doi.org/10.1021/jacs.2c04658.
(21) Aly, S.; El-Boraey, H. A. Effect of Gamma Irradiation on Spectral, XRD, SEM, DNA Binding, Molecular Modling and Antibacterial Property of Some (Z) N-(Furan-2-Yl)Methylene)-2-(Phenylamino)Acetohydrazide Metal(II) Complexes. *J. Mol. Struct.* **2019**, *1185*, 323–332. https://doi.org/10.1016/j.molstruc.2019.02.069.
(22) Sharma, K. K.; Singh, R.; Fahmi, N.; Singh, R. V. Synthesis, Coordination Behavior, and Investigations of Pharmacological Effects of Some Transition Metal Complexes with Isoniazid Schiff Bases. *J. Coord. Chem.* **2010**, *63* (17), 3071–3082. https://doi.org/10.1080/00958972.2010.504986.
(23) Hosny, N. M.; Sherif, Y. E. Synthesis, Structural, Optical and Anti-Rheumatic Activity of Metal Complexes Derived from (E)-2-Amino-N-(1-(2-Aminophenyl)Ethylidene)Benzohydrazide (2-AAB) with Ru(III), Pd(II) and Zr(IV). *Spectrochim. Acta. A. Mol. Biomol. Spectrosc.* **2015**, *136*, 510–519. https://doi.org/10.1016/j.saa.2014.09.064.
(24) Pradhan, S.; John, R. P. Self-Assembled Pd_6L_4 Cage and Pd_4L_4 Square Using Hydrazide Based Ligands: Synthesis, Characterization and Catalytic Activity in Suzuki–Miyaura Coupling Reactions. *RSC Adv.* **2016**, *6* (15), 12453–12460. https://doi.org/10.1039/C6RA00055J.
(25) Palla, G.; Predieri, G.; Domiano, P.; Vignali, C.; Turner, W. Conformational Behaviour and / Isomerization of -Acyl and -Aroylhydrazones. *Tetrahedron* **1986**, *42* (13), 3649–3654. https://doi.org/10.1016/S0040-4020(01)87332-4.
(26) Arya, N.; Mishra, S. K.; Suryaprakash, N. Intramolecular Hydrogen Bond Directed Distribution of Conformational Populations in the Derivatives of *N'*-Benzylidenebenzohydrazide. *New J. Chem.* **2019**, *43* (33), 13134–13142. https://doi.org/10.1039/C9NJ03071A.
(27) Kitamura, F.; Sawaguchi, K.; Mori, A.; Takagi, S.; Suzuki, T.; Kobayashi, A.; Kato, M.; Nakajima, K. Coordination Structure Conversion of Hydrazone–Palladium(II) Complexes in the Solid State and

in Solution. *Inorg. Chem.* **2015**, *54* (17), 8436–8448. https://doi.org/10.1021/acs.inorgchem.5b01128.
(28) Becke, A. D. Density-functional Thermochemistry. III. The Role of Exact Exchange. *J. Chem. Phys.* **1993**, *98* (7), 5648–5652. https://doi.org/10.1063/1.464913.